Universiteit
Leiden
The Netherlands

In vivo biomechanics of cruciate ligament injuries

Van de Velde, S.K.

Citation
Van de Velde, S. K. (2016, November 29). *In vivo biomechanics of cruciate ligament injuries*. Retrieved from https://hdl.handle.net/1887/44484

Version:	Not Applicable (or Unknown)
License:	Licence agreement concerning inclusion of doctoral thesis in the Institutional Repository of the University of Leiden
Downloaded from:	https://hdl.handle.net/1887/44484

Note: To cite this publication please use the final published version (if applicable).

Cover Page

Universiteit Leiden

The handle http://hdl.handle.net/1887/44484 holds various files of this Leiden University dissertation.

Author: Van de Velde, S.K.
Title: In vivo biomechanics of cruciate ligament injuries
Issue Date: 2016-11-29

5

CHAPTER

Increased tibiofemoral cartilage contact deformation in patients with anterior cruciate ligament deficiency.

Samuel K. Van de Velde
Jeffrey T. Bingham
Ali Hosseini
Michal Kozanek
Louis E. DeFrate
Thomas J. Gill, IV
Guoan Li

Arthritis Rheum. 2009 Dec;60(12):3693-702.

ABSTRACT

Objective. To investigate the in vivo cartilage contact biomechanics of the tibiofemoral joint following anterior cruciate ligament (ACL) injury.

Methods. Eight patients with an isolated ACL injury in 1 knee, with the contralateral side intact, participated in the study. Both knees were imaged using a specific magnetic resonance sequence to create 3- dimensional models of knee bone and cartilage. Next, each patient performed a lunge motion from 0° to 90° of flexion as images were recorded with a dual fluoroscopic system. The three-dimensional knee models and fluoroscopic images were used to reproduce the in vivo knee position at each flexion angle. With this series of knee models, the location of the tibiofemoral cartilage contact, size of the contact area, cartilage thickness at the contact area, and magnitude of the cartilage contact deformation were compared between intact and ACL- deficient knees.

Results. Rupture of the ACL changed the cartilage contact biomechanics between 0° and 60° of flexion in the medial compartment of the knee. Compared with the contralateral knee, the location of peak cartilage contact deformation on the tibial plateaus was more posterior and lateral, the contact area was smaller, the average cartilage thickness at the tibial cartilage contact area was thinner, and the resultant magnitude of cartilage contact deformation was increased. Similar changes were observed in the lateral compartment, with increased cartilage contact deformation from 0° to 30° of knee flexion in the presence of ACL deficiency.

Conclusion. ACL deficiency alters the in vivo cartilage contact biomechanics by shifting the contact location to smaller regions of thinner cartilage and by increasing the magnitude of the cartilage contact deformation.

INTRODUCTION

Many experts have abandoned the long-held belief that knee osteoarthritis (OA) is a straightforward "wear and tear" disease of cartilage.[1] Instead, the metabolic and structural changes of OA are currently viewed as the adaptive response of synovial joints to a variety of genetic, constitutional, or biomechanical insults.[2] Nevertheless, it remains widely accepted that knee joint instability is an important risk factor in the pathogenesis of the disease.[3,4,5]

The assumption that abnormal kinematics and consequent abnormal loading within the joint initiate knee OA underlies much of current OA research and orthopedic practice. Transection of the anterior cruciate ligament (ACL) is a well-established technique for inducing OA in animal models.[6,7] Reconstruction of the ruptured ACL has become one of the most frequently performed orthopedic procedures in an attempt to restore normal joint motion and prevent long-term complications.[3] A number of alignment-modifying therapeutic options, including bracing and osteotomy, might be used to alter the rate of OA progression.[8]

However, even though OA is widely believed to result in part from local mechanical factors acting within the context of systemic susceptibility, little is known about the extent of the mechanical alteration in the knee joint following rupture of the ACL. In general, the changes in kinematics that are observed in unstable knee joints are very minimal, on the order of millimeters.[9,10,11] Yet, these minimal alterations in kinematics are believed to trigger the devastating destruction of the articular cartilage.

Measuring articular cartilage function in the human knee joint with an acceptable degree of accuracy is technically challenging. The morphology of knee joint cartilage has been extensively investigated in knee specimens from cadaver donors and from living donors, using various techniques, such as needle probes, ultrasound, stereophotogrammetry, and magnetic resonance imaging (MRI).[12–18] Several recent studies have presented data on tibiofemoral contact kinematics in living subjects. Both open and closed MRI techniques have been used to determine tibiofemoral contact areas and locations for a variety of activities.[19,20,21] Other investigators have used a combination of either computed tomography (CT) or MRI with fluoroscopy to estimate cartilage contact locations during a lunge motion in healthy[22,23] and ACL-deficient[24,25] knees. In general, the cartilage contact location in these studies has been estimated based on the closest interarticular distance between the bony surfaces of the tibiofemoral joint[24] or the centroid of the tibiofemoral cartilage contact area.[25] While these previous studies have provided valuable data on the cartilage contact location, essential in vivo cartilage contact biomechanics, such as cartilage contact area, cartilage thickness, and cartilage contact deformation in a knee joint at risk of developing OA, remain unclear.

We hypothesized that rupture of the ACL changes the cartilage contact biomechanics of the tibiofemoral joint, with a resultant increase in the magnitude of cartilage contact deformation. In the present study, we used a combined dual fluoroscopic and MRI technique to analyze the effects of ACL deficiency on the location of tibiofemoral cartilage contact, the size of the contact area, the cartilage thickness at the contact area, and the magnitude of cartilage contact deformation during in vivo weight-bearing flexion of the knee from 0° to 90°.

PATIENTS AND METHODS

Patient selection. Eight patients (5 men and 3 women; age range 19–38 years) with complaints of knee laxity were included in the study. These patients had a diagnosis of acute, isolated ACL rupture, as documented by clinical examination findings (8-mm Lachman test with no end point, a grade 2 pivot-shift test measured by the same orthopedic surgeon [TJG], mean ± SD International Knee Documentation Committee[26] score 63.5 ± 8.7, mean ± SD manual maximum injured–minus–intact knee displacement score 4.2 ± 1.9 mm as measured with a KT-1000 knee ligament arthrometer [MEDmetric, San Diego, CA] by the same physical therapist) and findings on MRI. All patients had healthy contralateral knees. Patients had been injured within a mean ± SD of 4.4 ± 3 months of testing. Patients with injury to other ligaments, noticeable cartilage lesions, meniscal damage, and injury to the underlying bone were excluded from the study.

Five of these 8 patients were included in our previous studies of the 6 degrees-of-freedom tibiofemoral kinematics[9] as well as the motion of the tibiofemoral cartilage contact points in patients with ACL deficiency.[25] Each patient signed a consent form that had been approved by our Institutional Review Board.

Imaging procedure. The MRI and dual orthogonal fluoroscopic imaging techniques have been described in detail previously.[9,25,27] Briefly, both the left and the right knees were imaged with an MR scanner to create 3-dimensional (3-D) meshed models of the knees, using a protocol established in our laboratory.[9] To reduce the effects of load history on cartilage thickness, patients were asked to refrain from all strenuous activity, such as lifting, running, or stair climbing, for at least 4 hours prior to their visit and to remain non–weight bearing for ~1 hour prior to MRI of the knee. Patients were asked to lie supine, with the knee in a relaxed, extended position while sagittal plane images were acquired with a 3T MRI scanner (Siemens, Malvern, PA). The MR scanner was equipped with a surface coil and used a 3-D double-echo water excitation sequence (field of view 16 x 16 x 12 cm, voxel resolution 0.31 x 0.31 x 1.00 mm, repetition time [TR] 24 msec, echo time [TE] 6.5 msec, and flip angle 25°). Each scan lasted for ~12 minutes. The images were then imported into solid modeling software (Rhinoceros; Robert McNeel and Associates, Seattle, WA) to construct 3-D surface mesh models of the tibia, fibula, femur, and

articulating cartilage. The meshes were assembled using a point density of 80 vertices/cm^2 and triangular facets, with an average aspect ratio of 2.

After the MRI-based computer models were constructed, both knees of each patient were simultaneously imaged using 2 orthogonally placed fluoroscopes (OEC 9800; GE Healthcare, Salt Lake City, UT) as the patient performed a single-leg quasistatic lunge at 0°, 15°, 30°, 60°, and 90° of flexion. At each flexion angle, the patient was asked to pause for 5 seconds while simultaneous fluoroscopic images were taken. Throughout the experiment, the leg being tested supported the patient's body weight, while the other leg provided stability. The time elapsed between the MRI scan and the lunge activity was ~15 minutes.

Next, the fluoroscopic images were imported into solid modeling software and placed in the orthogonal planes based on the position of the fluoroscopes during imaging of the patient. Finally, the 3-D MRI–based knee model of each patient was imported into the same software, viewed from the 2 orthogonal directions corresponding to the orthogonal fluoroscopic setup used to acquire the images, and independently manipulated in 6 degrees of freedom inside the software until the projections of the model matched the outlines of the fluoroscopic images. When the projections matched the outlines of the images taken during in vivo knee flexion, the model reproduced the in vivo position of the knee. This system has an error of <0.1 mm and 0.3° in measuring tibiofemoral joint translations and rotations, respectively.[9] When comparing the dual fluoroscopic model matching technique with tantalum bead matching, a technique similar to Roentgen stereophotogrammetric analysis, the difference between the 2 techniques in the proximodistal direction (i.e., analogous to the measured apparent penetration) was 0.075 ± 0.13 mm (mean ± SD).[28]

Statistical analysis. In this study, cartilage thickness was calculated by finding the smallest Euclidian distance connecting a vertex of the articular surface to the cartilage–bone interface of the 3-D surface mesh models. The size of the contact area between the tibia and femur was determined by computing the area of tibial cartilage that intersected the femoral cartilage.[27] The cartilage contact deformation was then defined for each vertex of the articular surface mesh as the amount of cartilage surface intersection (in mm) (Figure 1) divided by the sum of the tibial and femoral cartilage surface thicknesses (in mm) multiplied by 100.[27] In this study, cartilage contact location was defined as the location of peak cartilage deformation, referenced to Cartesian coordinate systems on the tibial plateaus[23,25,29] (Figure 2). The origin of each coordinate system was located at the center of a circle, which was fit to the posterior edge of each tibial compartment. The anteroposterior and mediolateral axes split each tibial plateau into quadrants. In the anteroposterior direction, a location anterior to the mediolateral axis was considered positive. In the mediolateral direction, a location lateral to the anteroposterior axis was considered positive.

In a recent study of in vivo cartilage contact deformation in the healthy human tibiofemoral joint, a lack of agreement of 14 ± 11% (mean ± SD) was found between the combined dual fluoroscopic–MRI technique and a silicone casting technique in calculating the mean ± SD cartilage contact area of 244 ± 131 mm^2.[27] For the present study, we conducted an accuracy and precision analysis of the tibiofemoral cartilage reconstructions in which the measurement of cartilage thickness based on 3-D MRI–based knee models was compared with direct cartilage thickness measurement on calibrated digital images of cross-sections of specimens from the cadaver donors, and repeatedly measured for intra- and interobserver precision (see Appendix A). The average absolute difference between the cartilage thickness values based on the 3-D MRI–based knee models and those captured from the specimens from the cadaver donors was 0.04 ± 0.01 mm (mean ± SD), and excellent intra- and interobserver precision was obtained.

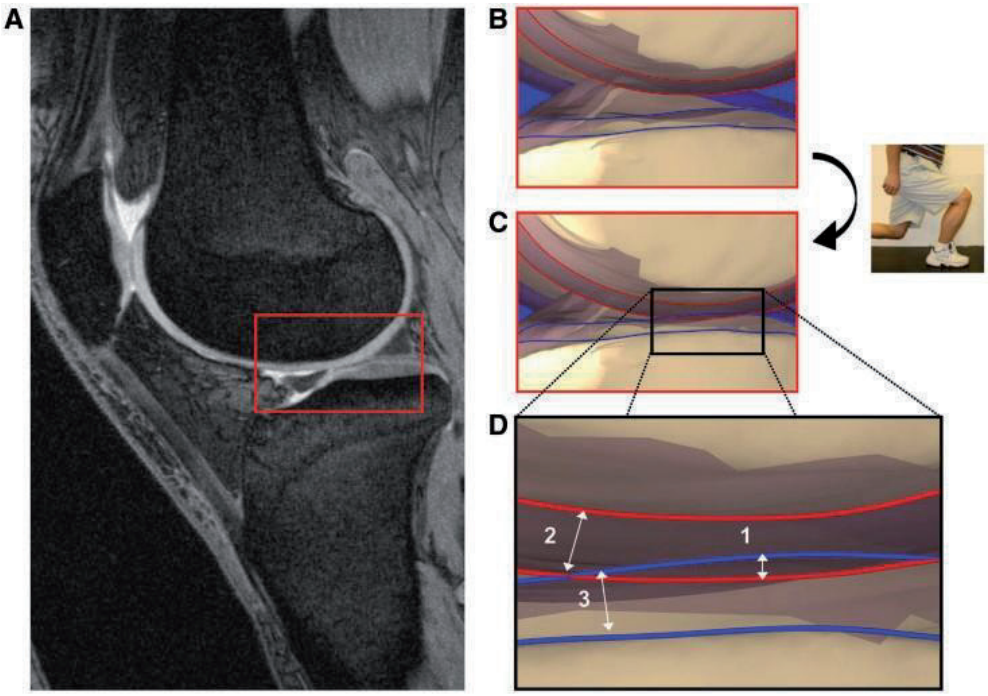

Figure 1. Illustration of the calculation of compartmental contact deformation. The MR images of the knee joint after ~1 h non-weight bearing (**A**) are used to determine the respective cartilage thicknesses of the femur (red outlines) and tibia (blue outlines) at rest (**B**). After matching the MR models to the fluoroscopic images captured during weight-bearing lunge (**C**), compartmental cartilage deformation is calculated by dividing the amount of penetration (1) by the sum of the femoral (2) and tibial (3) cartilage surface thicknesses, as illustrated in (**D**).

A two-way repeated-measures analysis of variance and the Student-Newman-Keuls post hoc test were used to determine statistically significant differences in location, contact area, thickness, and cartilage contact deformation between the intact contralateral knees and the ACL-deficient knees at each flexion angle. *P* values less than 0.05 were considered significant.

RESULTS

Location of cartilage contact. In general, the location of peak cartilage contact deformation on the tibial plateaus was more posterior and lateral in ACL-deficient knees as compared with healthy contralateral knees. In the medial compartment of ACL-deficient knees, cartilage contact shifted posteriorly by an average (±SD) of 6.3 ± 0.7 mm at 0° and 15° of flexion (Figure 2A) and laterally by an average of 4.7 ± 0.9 mm between 0° and 60° of flexion (Figure 2B), as compared with the location in the intact knees. In the lateral compartment, cartilage contact shifted posteriorly by an average of 3.6 ± 1.3 mm between 0° and 30° of flexion (Figure 2C) and shifted laterally by an average of 4.2 ± 0.6 mm between 0° and 60° of flexion (Figure 2D) following rupture of the ACL.

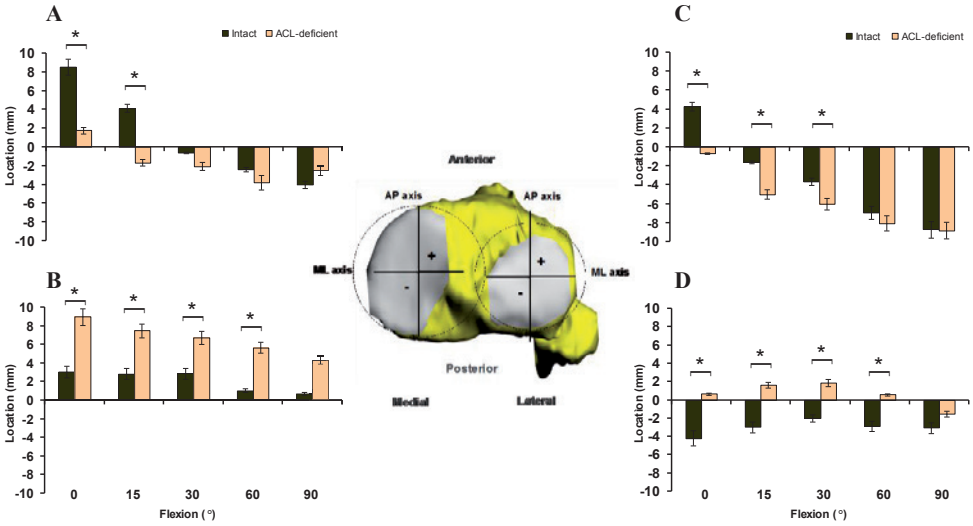

Figure 2. Location of cartilage contact on the medial tibial plateau in the anteroposterior (AP) (**A**) and mediolateral (ML) (**B**) directions and on the lateral tibial plateau in the AP (**C**) and ML (**D**) directions in intact and anterior cruciate ligament (ACL)-deficient knees as a function of knee flexion angle in 8 patients with acute, isolated rupture of the ACL. The central illustration shows the Cartesian coordinate system on the tibial plateau. Values are the mean ± SD. * = $P < 0.05$.

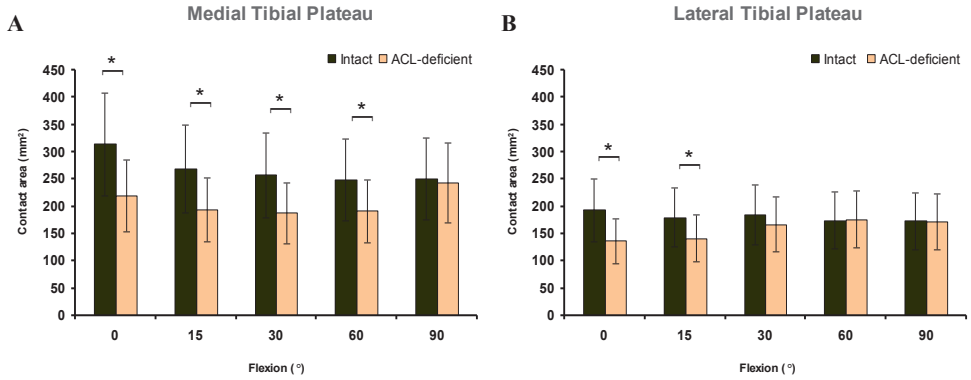

Figure 3. Cartilage contact area on the medial (**A**) and lateral (**B**) tibial plateaus in intact and anterior cruciate ligament (ACL)-deficient knees as a function of knee flexion angle in 8 patients with acute, isolated rupture of the ACL. Values are the mean ± SD. * = $P < 0.05$.

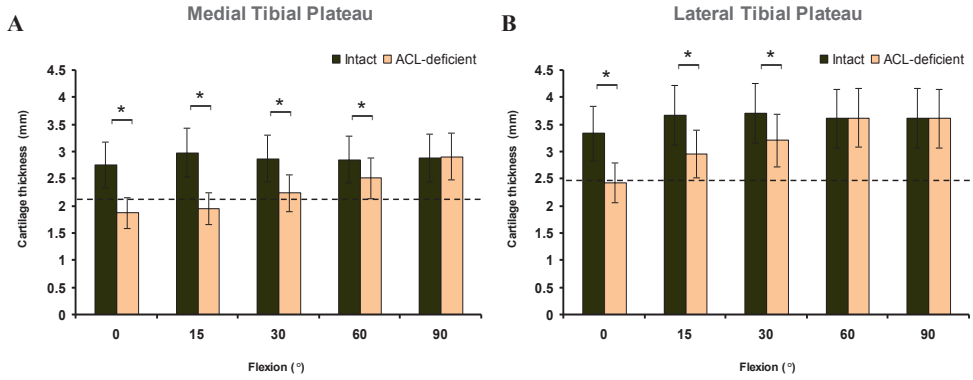

Figure 4. Thickness of cartilage in regions of contact on the medial (**A**) and lateral (**B**) tibial plateaus in intact and anterior cruciate ligament (ACL)-deficient knees as a function of knee flexion angle in 8 patients with acute, isolated rupture of the ACL. Values are the mean ± SD. * = $P < 0.05$.

Size of the contact area. In the medial compartment, the cartilage contact area in ACL-deficient knees was significantly smaller from 0° to 60° of flexion ($P < 0.05$) than that in the intact knees (Figure 3A). The maximum decrease in cartilage contact area after ACL rupture occurred at 0° of flexion (219.6 ± 69.4 mm^2 in the ACL-deficient knee versus 314.4 ± 113.6 mm^2 in the intact knee; $P = 0.0025$). In the lateral compartment, a decrease in contact area in ACL-deficient knees was observed at the lowest flexion angles (137.1 ±

64.1 mm^2 and 141.7 ± 48.7 mm^2 at 0° and 15° of flexion, respectively, in ACL-deficient knees versus 193.4 ± 75.2 mm^2 and 180.0 ± 46.8 mm^2, respectively, in intact knees [P = 0.0004 and P = 0.0041, respectively]) (Figure 3B).

Cartilage thickness at the contact area. The total average thickness of cartilage in the studied knees was 2.2 ± 0.4 mm (mean ± SD) and 2.5 ± 0.5 mm, respectively, in the medial and lateral tibial plateaus. In the intact contralateral knees, the cartilage thickness located in areas of contact was an average of 1.4 times greater than the total average thickness. In contrast, regions of contact for both the medial and lateral compartments in ACL-deficient knees were an average of 0.9 times thinner than the total average thickness. Cartilage thickness at contact was an average of 0.7 ± 0.3 mm thinner between 0° and 60° of flexion in the medial compartment (Figure 4A) and 0.7 ± 0.2 mm thinner between 0° and 30° of flexion in the lateral compartment (Figure 4B) as compared with the cartilage thickness at contact in the respective compartments of intact knees.

Magnitude of cartilage contact deformation. Rupture of the ACL significantly increased the deformation of cartilage between 0° and 60° of flexion in the medial compartment of the knee joint as compared with the intact knees (P < 0.05) (Figure 5A). The maximum increase in compartmental cartilage deformation after ACL rupture occurred at 0° of flexion (19 ± 4% intact knee, 29 ± 9% ACL-deficient knee, P = 0.0138). The increase in cartilage deformation that was observed after ACL rupture gradually lessened with flexion. At 90° of flexion, there was no significant difference in cartilage deformation between the healthy and ACL-deficient knee.

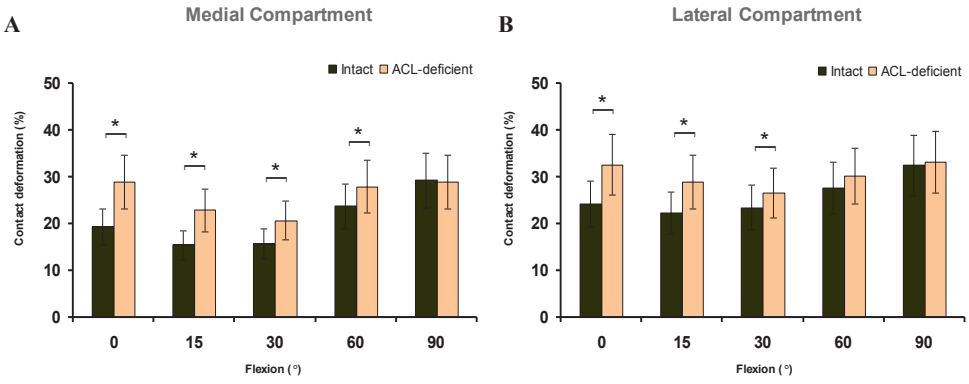

Figure 5. Peak cartilage contact deformation in the medial (**A**) and lateral (**B**) tibiofemoral compartments in intact and anterior cruciate ligament (ACL)-deficient knees as a function of knee flexion angle in 8 patients with acute, isolated rupture of the ACL. Values are the mean ± SD. * = P < 0.05.

In the lateral compartment, rupture of the ACL significantly increased the deformation of cartilage between 0° and 30° of knee flexion ($P < 0.05$) (Figure 5B). The maximum increase in cartilage deformation after ACL rupture occurred at 0° of flexion, where a mean ± SD percentage deformation of 24 ± 9% was found in the healthy knee and 33 ± 6% in the ACL-deficient knee ($P = 0.0033$).

DISCUSSION

Rupture of the ACL mostly affects patients under 30 years of age[30] and is associated clinically with an increased incidence,[3,4] an earlier onset,[4] and a faster progression[31] of knee OA. In vivo T1ρ quantitative assessment of knee cartilage after ACL injury using 3T MRI has previously demonstrated that cartilage abnormalities were already present following initial ACL injury in patients with underlying bone marrow edema–like lesions in the lateral tibia,[15] suggesting a role in the pathogenesis of OA in ACL deficiency.[32,33] Interestingly though, an increased prevalence of cartilage degeneration has been described in the medial compartment in the presence of an ACL injury,[34–37] whereas the bone marrow edema–like lesions are usually found in the lateral compartment of the knee.[38]

Based on theoretical models, it has been hypothesized that the persistent abnormal kinematic behavior that is seen in isolated ACL deficiency could alter the stress distributions in the cartilage over time, thereby predisposing the knee to degenerative changes.[39] This "wear and tear" theory could be supported by the efficacy of the classic animal models of knee OA, in which transection of the ACL, with consequent joint instability, but without injury to the other structures of the knee, triggers cartilage degeneration.[40,41] However, it remains poorly understood how, during in vivo weightbearing flexion of the knee, the minimal changes in cartilage contact kinematics observed in unstable knee joints without manifest initial cartilage or underlying bone lesions[25] could contribute to the initiation of OA.

In our previous in vivo analysis of the tibiofemoral joint kinematics in patients with ACL deficiency, we found an increased anterior translation (~3 mm) and internal rotation (~2°) of the tibia at low flexion angles as compared with the healthy control knee.[9] Similar findings have been well documented in the literature.[10,11] ACL deficiency also caused an increased medial tibial translation of ~1 mm. These changes in tibiofemoral kinematics after ACL injury were expected to lead to changes in the tibiofemoral cartilage contact characteristics. Specifically, the medial shift of the tibia after ACL deficiency would alter the contact stress distributions in the tibiofemoral cartilage near the medial tibial spine. Indeed, in the presence of ACL injury, the cartilage contact points shifted not only posteriorly, as was expected based on the increased anterior tibial translation, but also laterally on the surface of the tibial plateau.[25] In the medial compartment, the contact points shift toward the medial tibial spine, a region where degeneration is observed in patients

with chronic ACL injuries.[34] The question remained as to whether the ~2-mm shift in cartilage contact (determined based on the location of the centroid of the cartilage contact area) to incongruent articular regions of the knee joint affects the stress on the cartilage of the joint.

In the present study, we found a similar posterior and lateral shift in cartilage contact location on the surface of the tibial plateaus following ACL injury. However, when determining the location of cartilage contact based on the location where peak cartilage deformation occurred, we found that the magnitude of the posterior and lateral shift following ACL rupture (~5 mm) was greater than that previously reported.[25] A possible explanation for the discrepancy in the magnitude of shift based on measurement methodology could be found in the regional variations in cartilage thickness. When determining the cartilage contact location based on the closest interarticular distance between the bony surfaces of the tibiofemoral joint[24] or the centroid of the tibiofemoral cartilage contact area,[25] regional variations in the thickness of underlying cartilage are not taken into account. In the present study, the region of tibiofemoral cartilage contact was not only smaller following rupture of the ACL, but also had significantly thinner cartilage at contact in both the medial and lateral compartments as compared with the thickness at contact in the intact knees. In other words, the minimal shift in the location of the cartilage contact area to regions of thinner cartilage as reported previously[25] resulted in a considerable change in cartilage loading distribution within the knee joint.

The posterior and lateral shift in cartilage contact to thinner articular regions increased the magnitude of cartilage deformation in those regions. The maximum relative increase in cartilage contact deformation after ACL rupture occurred at full extension in the medial compartment, where deformation of 19 ± 4% was found in healthy knees and 29 ± 9% in ACL-deficient knees as compared with deformation of 24 ± 9% and 33 ± 6%, respectively, in the lateral compartment. The relatively greater increase in cartilage deformation in the medial compartment as compared with the lateral compartment relates to the increased development of OA in the medial compartment of the knee joint, as was observed during arthroscopic examination of 130 ACL-deficient patients.[35]

Due to the constraints of the imaging technique, motion and deformation of the meniscus were not detectable in the fluoroscopic images. For quantitative examination of the interaction of molecular changes in the meniscus and adjacent cartilage in ACL deficiency, recent developments in MRI techniques, such as T1ρ mapping, represent potential means.[42] However, based on our previous validation of the imaging technique,[27] the present limitation in examination of the meniscus by the dual fluoroscopic technique did not affect the determination of cartilage–cartilage contact, since articular surface mesh penetration was only recorded at the location of in vivo tibiofemoral cartilage contact. An additional constraint of the present methodology is that any possible underlying physiochemical activities (e.g., elevated cytokines in the joint fluid[43]) that might occur in the knee joint

following ACL rupture could not be analyzed, thereby restricting the formulation of inclusive insight into the pathogenesis of OA in knee joint instability. In addition, regional variations in the mechanical properties of the articular cartilage were not taken into account when computing the cartilage contact deformation. This may be a limitation, since in vitro compression of tibial cartilage explants obtained from distinct regions of the joint has demonstrated that chondrocytes displayed region-specific baseline gene expression and responded differently to in vitro mechanical loading.[44]

Patients with discernible cartilage lesions on 3T MRI at a mean ± SD of 4.5 ± 3 months of injury were excluded from the study. However, with our methodology, we were unable to appreciate the extent of potential cartilage softening that existed at the time of the analysis and were thus unable to resolve the "chicken-or-egg" issue. Were our measured deformation differentials attributable to the ACL-deficient knee cartilage being more compliant, rather than increased deformation being responsible for the subsequent degeneration onset? Future studies using a methodology similar to that used in this pilot study, with baseline and follow-up imaging biomarkers, such as T1ρ or delayed gadolinium-enhanced MRI of cartilage, should follow ACL-deficient patients who are treated conservatively for longer periods. Tibiofemoral contact deformation and the health of the cartilage could therefore be monitored over time to quantify any possible biomechanical relationships.

We acquired data from only 1 functional activity, a single leg lunge, using a goniometer to measure the flexion angle. Measurement of the forces and strains in human tissues is currently impracticable, which impedes the extrapolation of the current findings to other weightbearing activities. It is conceivable that the knee joint anteroposterior shear forces during the single leg lunge might be higher than during normal gait,[45] thus exaggerating the measured articular surface engagement differentials. However, it has been reported that the magnitude of the anteroposterior shear forces increase with knee flexion during the descent phase of a lunge performed with a 223-N (50-lb) barbell[46] and that the knee forces are minimal in the functional range between 0° and 50° of knee flexion.[47] In the present study, the largest deformation differential was observed around 0° of knee flexion. In future studies, other in vivo activities, such as walking, running, and stair climbing, should be considered in order to construct a comprehensive insight into the effect of ACL deficiency on cartilage during daily activities.

During performance of the lunge activity, our patients were asked to pause for 5 seconds at each flexion angle while simultaneous fluoroscopic images were taken. To the best of our knowledge, the real-time in vivo creep of tibiofemoral cartilage has not yet been studied. Based on the in vivo creep compression curves for ankle cartilage using similar assessment methodologies which showed that cartilage contact deformation continued to increase during the first 20 seconds of loading,[48] it might be possible that the present data represent a

conservative estimate of a potentially bigger differential if the patients were asked to pause longer at each flexion angle.

It should be noted that no ground reaction forces were measured in this study to document that global knee joint loading was replicated reproducibly for both the intact and the ACL-deficient knee. The patient performed the lunge activity with full body weight on the tested leg, while the untested leg was used for balance only, to ensure physiologic loading conditions.

Finally, the present analysis compared tibiofemoral cartilage contact deformation in ACL-deficient and intact knees at each flexion angle, thereby ignoring potential interactions among the measured cartilage deformation and various knee flexion angles. Further research involving a larger study sample needs to be performed to confirm the present findings. Nonetheless, we believe our results provided comprehensible insight into the changes in in vivo tibiofemoral cartilage contact deformation following injury of the ACL and identified important directions for future research.

We found that rupture of the ACL alters the in vivo cartilage contact biomechanics of the tibiofemoral joint by shifting the cartilage contact location to smaller regions of thinner cartilage and increasing the magnitude of cartilage contact deformation.

REFERENCES

1. Aspden RM, Scheven BA, Hutchison JD. Osteoarthritis as a systemic disorder including stromal cell differentiation and lipid metabolism. Lancet 2001;357:1118–20.
2. Brandt K, Lohmander L, Doherty M. The concept of osteoarthritis as failure of the diarthrodial joint. In: Brandt K, Doherty M, Lohmander L, editors. Osteoarthritis. Oxford: Oxford University Press; 1998. p. 70–4.
3. Fithian DC, Paxton LW, Goltz DH. Fate of the anterior cruciate ligament-injured knee. Orthop Clin North Am 2002;33:621–36, v.
4. Roos H, Adalberth T, Dahlberg L, Lohmander LS. Osteoarthritis of the knee after injury to the anterior cruciate ligament or meniscus: the influence of time and age. Osteoarthritis Cartilage 1995;3:261–7.
5. Felson DT, Lawrence RC, Dieppe PA, Hirsch R, Helmick CG, Jordan JM, et al. Osteoarthritis: new insights. Part 1: the disease and its risk factors [review]. Ann Intern Med 2000;133:635–46.
6. Marshall KW, Chan AD. Arthroscopic anterior cruciate ligament transection induces canine osteoarthritis. J Rheumatol 1996;23: 338–43.
7. Brandt KD, Myers SL, Burr D, Albrecht M. Osteoarthritic changes in canine articular cartilage, subchondral bone, and synovium fifty-four months after transection of the anterior cruciate ligament. Arthritis Rheum 1991;34:1560–70.
8. Hunter DJ, Sharma L, Skaife T. Alignment and osteoarthritis of the knee. J Bone Joint Surg Am 2009;91 Suppl 1:85–9.
9. DeFrate LE, Papannagari R, Gill TJ, Moses JM, Pathare NP, Li G. The 6 degrees of freedom kinematics of the knee after anterior cruciate ligament deficiency: an in vivo imaging analysis. Am J Sports Med 2006;34:1240–6.
10. Georgoulis AD, Papadonikolakis A, Papageorgiou CD, Mitsou A, Stergiou N. Three-dimensional tibiofemoral kinematics of the anterior cruciate ligament-deficient and reconstructed knee during walking. Am J Sports Med 2003;31:75–9.
11. Logan M, Dunstan E, Robinson J, Williams A, Gedroyc W, Freeman M. Tibiofemoral kinematics of the anterior cruciate ligament (ACL)-deficient weightbearing, living knee employing vertical access open "interventional" multiple resonance imaging. Am J Sports Med 2004;32:720–6.
12. Shepherd DE, Seedhom BB. Thickness of human articular cartilage in joints of the lower limb. Ann Rheum Dis 1999;58:27–34.
13. Jones G, Glisson M, Hynes K, Cicuttini F. Sex and site differences in cartilage development: a possible explanation for variations in knee osteoarthritis in later life. Arthritis Rheum 2000;43:2543–9.
14. Ateshian GA, Soslowsky LJ, Mow VC. Quantitation of articular surface topography and cartilage thickness in knee joints using stereophotogrammetry. J Biomech 1991;24:761–76.

15. Bolbos RI, Ma CB, Link TM, Majumdar S, Li X. In vivo T1p quantitative assessment of knee cartilage after anterior cruciate ligament injury using 3 Tesla magnetic resonance imaging. Invest Radiol 2008;43:782–8.

16. Saadat E, Jobke B, Chu B, Lu Y, Cheng J, Li X, et al. Diagnostic performance of in vivo 3-T MRI for articular cartilage abnormalities in human osteoarthritic knees using histology as standard of reference. Eur Radiol 2008;18:2292–302.

17. Samosky JT, Burstein D, Eric Grimson W, Howe R, Martin S, Gray ML. Spatially-localized correlation of dGEMRIC-measured GAG distribution and mechanical stiffness in the human tibial plateau. J Orthop Res 2005;23:93–101.

18. Taylor C, Carballido-Gamio J, Majumdar S, Li X. Comparison of quantitative imaging of cartilage for osteoarthritis: T2, T1p, dGEMRIC and contrast-enhanced computed tomography. Magn Reson Imaging 2009:27:779–84.

19. Freeman MA, Pinskerova V. The movement of the knee studied by magnetic resonance imaging. Clin Orthop Relat Res 2003: 35–43.

20. Hinterwimmer S, Gotthardt M, von Eisenhart-Rothe R, Sauerland S, Siebert M, Vogl T, et al. In vivo contact areas of the knee in patients with patellar subluxation. J Biomech 2005;38:2095–101.

21. Wretenberg P, Ramsey DK, Nemeth G. Tibiofemoral contact points relative to flexion angle measured with MRI. Clin Biomech (Bristol, Avon) 2002;17:477–85.

22. Asano T, Akagi M, Tanaka K, Tamura J, Nakamura T. In vivo three-dimensional knee kinematics using a biplanar image-matching technique. Clin Orthop 2001:157–66.

23. Li G, DeFrate LE, Park SE, Gill TJ, Rubash HE. In vivo articular cartilage contact kinematics of the knee: an investigation using dual-orthogonal fluoroscopy and magnetic resonance image-based computer models. Am J Sports Med 2005;33:102–7.

24. Dennis DA, Mahfouz MR, Komistek RD, Hoff W. In vivo determination of normal and anterior cruciate ligament-deficient knee kinematics. J Biomech 2005;38:241–53.

25. Li G, Moses JM, Papannagari R, Pathare NP, DeFrate LE, Gill TJ. Anterior cruciate ligament deficiency alters the in vivo motion of the tibiofemoral cartilage contact points in both the antero-posterior and mediolateral directions. J Bone Joint Surg Am 2006;88:1826–34.

26. Irrgang JJ, Anderson AF, Boland AL, Harner CD, Kurosaka M, Neyret P, et al. Development and validation of the International Knee Documentation Committee subjective knee form. Am J Sports Med 2001;29:600–13.

27. Bingham JT, Papannagari R, Van de Velde SK, Gross C, Gill TJ, Felson DT, et al. In vivo cartilage contact deformation in the healthy human tibiofemoral joint. Rheumatology (Oxford) 2008; 47:1622–7.

28. Li G, Van de Velde SK, Bingham JT. Validation of a non-invasive fluoroscopic imaging technique for the measurement of dynamic knee joint motion. J Biomech 2008;41:1616–22.

29. Li G, Park SE, DeFrate LE, Schutzer ME, Ji L, Gill TJ, et al. The cartilage thickness distribution in the tibiofemoral joint and its correlation with cartilage-to-cartilage contact. Clin Biomech (Bristol, Avon) 2005;20:736–44.

30. Griffin LY, Agel J, Albohm MJ, Arendt EA, Dick RW, Garrett WE, et al. Noncontact anterior cruciate ligament injuries: risk factors and prevention strategies. J Am Acad Orthop Surg 2000; 8:141–50.

31. Kannus P, Jarvinen M. Posttraumatic anterior cruciate ligament insufficiency as a cause of osteoarthritis in a knee joint. Clin Rheumatol 1989;8:251–60.

32. Hernandez-Molina G, Guermazi A, Niu J, Gale D, Goggins J, Amin S, et al. Central bone marrow lesions in symptomatic knee osteoarthritis and their relationship to anterior cruciate ligament tears and cartilage loss. Arthritis Rheum 2008;58:130–6.

33. Li X, Ma BC, Bolbos RI, Stahl R, Lozano J, Zuo J, et al. Quantitative assessment of bone marrow edema-like lesion and overlying cartilage in knees with osteoarthritis and anterior cruciate ligament tear using MR imaging and spectroscopic imaging at 3 Tesla. J Magn Reson Imaging 2008;28:453–61.

34. Fairclough JA, Graham GP, Dent CM. Radiological sign of chronic anterior cruciate ligament deficiency. Injury 1990;21: 401–2.

35. Murrell GA, Maddali S, Horovitz L, Oakley SP, Warren RF. The effects of time course after anterior cruciate ligament injury in correlation with meniscal and cartilage loss. Am J Sports Med 2001;29:9–14.

36. Amin S, Guermazi A, LaValley MP, Niu J, Clancy M, Hunter DJ, et al. Complete anterior cruciate ligament tear and the risk for cartilage loss and progression of symptoms in men and women with knee osteoarthritis. Osteoarthritis Cartilage 2008;16:897–902.

37. Hill CL, Seo GS, Gale D, Totterman S, Gale ME, Felson DT. Cruciate ligament integrity in osteoarthritis of the knee. Arthritis Rheum 2005;52:794–9.

38. Fowler PJ. Bone injuries associated with anterior cruciate ligament disruption. Arthroscopy 1994;10:453–60.

39. Andriacchi TP, Mundermann A, Smith RL, Alexander EJ, Dyrby CO, Koo S. A framework for the in vivo pathomechanics of osteoarthritis at the knee. Ann Biomed Eng 2004;32:447–57.

40. Brandt KD. Transection of the anterior cruciate ligament in the dog: a model of osteoarthritis. Semin Arthritis Rheum 1991;21 Suppl 2:22–32.

41. Lozano J, Saadat E, Li X, Majumdar S, Ma CB. Magnetic resonance T(1ρ) imaging of osteoarthritis: a rabbit ACL transection model. Magn Reson Imaging 2009;27:611–6.

42. Bolbos RI, Link TM, Benjamin Ma C, Majumdar S, Li X. T1 ρ relaxation time of the meniscus and its relationship with T1 ρ of adjacent cartilage in knees with acute ACL injuries at 3 T. Osteoarthritis Cartilage 2009;16:12–8.

43. Cameron M, Buchgraber A, Passler H, Vogt M, Thonar E, Fu F, et al. The natural history of the anterior cruciate ligament-deficient knee. Changes in synovial fluid cytokine and keratin sulfate concentrations. Am J Sports Med 1997;25:751–4.

44. Bevill SL, Briant PL, Levenston ME, Andriacchi TP. Central and peripheral region tibial plateau chondrocytes respond differently to in vitro dynamic compression. Osteoarthritis Cartilage 2009;17: 980–7.

45. Shelburne KB, Torry MR, Pandy MG. Muscle, ligament, and joint-contact forces at the knee during walking. Med Sci Sports Exerc 2005;37:1948–56.

46. Stuart MJ, Meglan DA, Lutz GE, Growney ES, An KN. Comparison of intersegmental tibiofemoral joint forces and muscle activity during various closed kinetic chain exercises. Am J Sports Med 1996;24:792–9.

47. Escamilla RF. Knee biomechanics of the dynamic squat exercise. Med Sci Sports Exerc 2001;33:127–41.

48. Li G, Wan L, Kozanek M. Determination of real-time in-vivo cartilage contact deformation in the ankle joint. J Biomech 2008; 41:128–36.

49. Raynauld JP, Kauffmann C, Beaudoin G, Berthiaume MJ, de Guise JA, Bloch DA, et al. Reliability of a quantification imaging system using magnetic resonance images to measure cartilage thickness and volume in human normal and osteoarthritic knees. Osteoarthritis Cartilage 2003;11:351–60.

APPENDIX - ACCURACY AND PRECISION OF TIBIOFEMORAL CARTILAGE THICKNESS MEASUREMENT BY 3T MR IMAGING

Assessment of the accuracy and precision of cartilage thickness measurement based on 3-D meshed knee models created with 3T MR images is critical for the appreciation of biomechanical parameters such as in vivo cartilage contact deformation. In a validation study, we used calibrated digital images of a series of cartilage cross- sections from cadaver donors as the gold standard since the actual cartilage boundaries can be clearly delineated from the specimens (Figure A1 en A2).

Two fresh-frozen knee specimens from cadaver donors (right knee from a 48-year-old man; left knee from a 48-year-old woman) were selected. Specimens were stored at -20°C prior to testing and were thawed at room temperature for 24 hours before experimentation. Discernible cartilage damage in each specimen was ruled out by fluoroscopic, MRI, and visual examinations. Both knee specimens, with surrounding soft tissues intact, were then imaged with a 3T MRI scanner to create 3-D meshed models of the tibia, femur, and articulating cartilage layers using the protocol described previously.

Following MRI, the knee specimens were stripped of all surrounding soft tissues and disarticulated, leaving only the individual bones and articular cartilage surfaces. The bones were successively installed in a rigid cylinder with the shaft centered and osteotomized through the midsagittal planes of the articulating surfaces of the medial and lateral condyles. Between each osteotomy/digital image capturing of the pertinent cross-section, the specimens were wrapped in a moist dressing to prevent desiccation of the articular

cartilage. Eight cartilage cross-sections from the 2 specimens were measured (i.e., 2 cross-sections of each tibia and each femur). Digital images of the cross-sections were captured and were calibrated using a fluoroscopic image calibration protocol designed in our laboratory.

We next determined the same cross-section of the respective tibial and femoral cartilage layers in the 3-D surface mesh models. The osteotomized bones were CT scanned (LightSpeed Pro16 scanner; GE, Waukesha, WI). High-resolution axial-plane images were obtained (thickness 0.625 mm, gap 0.625 mm, and resolution 512 X 512 pixels). The CT images were then imported into MatLab (MathWorks, Natick, MA), and the contours of the osteotomized bones were digitized for each CT image based on a modified Canny edge detection method that combined pixel magnitude to construct a 3-D anatomic mesh model of the osteotomized bones. The osteotomized bone models were then mapped to the MRI-based models of the knee specimens using a customized code implemented in MatLab, based on the iterative closest point method. A plane was constructed along the cutting cross-section of the CT bone model. This plane was used to separate the MRI model at the location of the osteotomy.

The calibrated digital images of cartilage cross-sections were then matched to the respective cross-sectional planes of the MRI models. Thus, cartilage thickness could be measured at the same location on both the digital image and the MRI model. Ten equally distributed locations on each of the 8 cartilage cross-sections were measured and compared using Student's paired t-test, with significance set at $P < 0.05$.

For the first specimen, the average cartilage thickness values measured from the digital images versus the MRI models were 2.03 + 0.26 mm (mean + SD) versus 2.04 + 0.27 mm for the medial femoral condyle (absolute difference 0.05 + 0.03 mm; $P = 0.789$), 2.00 + 0.31 mm versus 2.02 + 0.30 mm for the lateral femoral condyle (absolute difference 0.05 + 0.03 mm; $P = 0.527$), 2.24 + 0.51 mm versus 2.26 + 0.48 mm for the medial tibial condyle (absolute difference 0.05 + 0.03 mm; $P = 0.378$), and 2.16 + 0.98 mm versus 2.18 + 1.00 mm for the lateral tibial condyle (absolute difference 0.04 + 0.03 mm; $P = 0.354$).

For the second specimen, the average cartilage thickness values measured from the digital images versus the MRI models were 2.15 + 0.29 mm versus 2.17 + 0.30 mm for the medial femoral condyle (absolute difference 0.04 + 0.03 mm; $P = 0.357$), 2.52 + 0.49 mm versus 2.52 + 0.48 mm for the lateral femoral condyle (absolute difference 0.03 + 0.02 mm; $P = 0.826$), 2.06 + 0.22 mm versus 2.04 + 0.23 mm for the medial tibial condyle (absolute difference 0.04 + 0.01 mm; $P = 0.447$), and 3.15 + 0.81 mm versus 3.17 + 0.80 mm for the lateral tibial condyle (absolute difference 0.03 + 0.02 mm; $P = 0.521$).

The average absolute difference in cartilage thickness, as measured at the 10 locations along the 8 section planes, between the direct measurement of the specimens and the MRI-based models was 0.04 + 0.01 mm (corresponding to a 1.8 + 1.6% difference). This

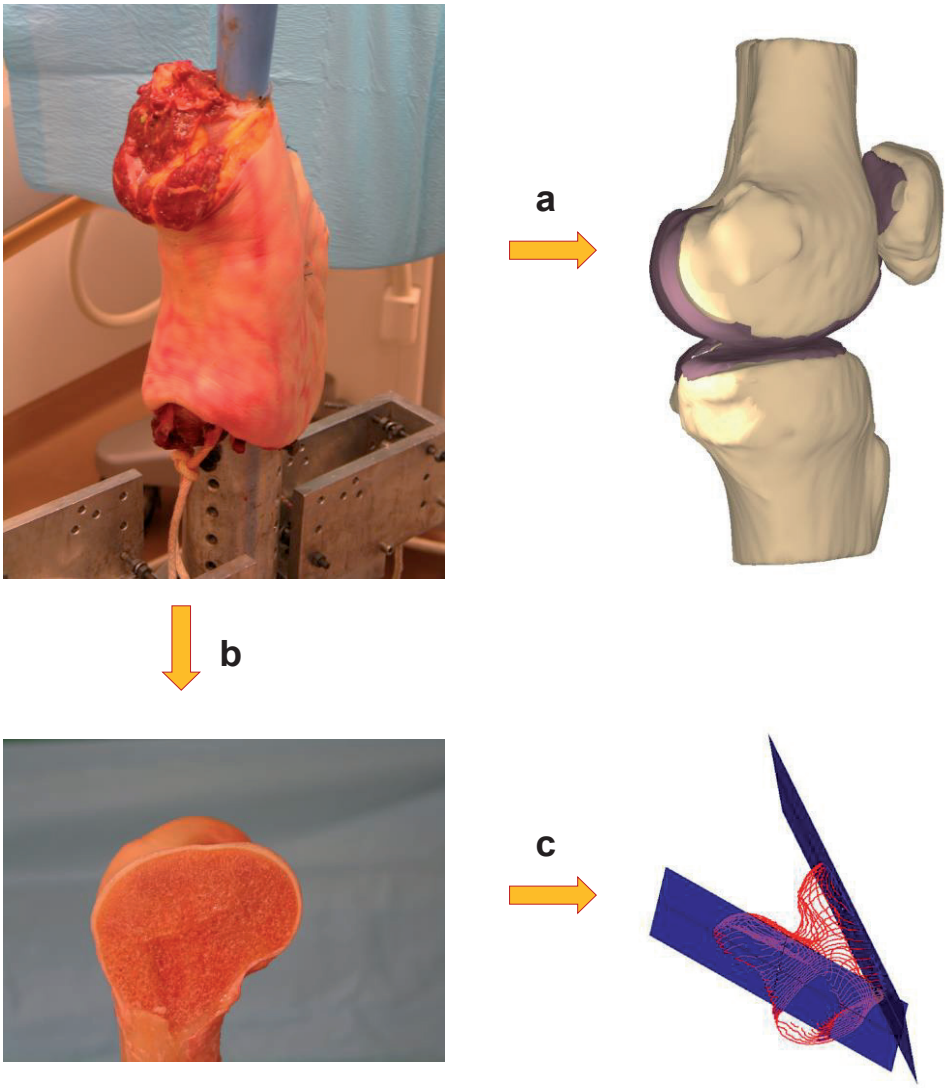

Figure A1. (**a**) 3T MR images were used to create 3D models of the cadaver knees; (**b**) digital images of osteotomized condyles were captured for gold standard measurement; (**c**) CT images of osteotomized bones were used to determine the location of the osteotomies.

demonstrated that the MRI-based cartilage model was close to the actual cartilage and was sufficiently accurate for the determination of cartilage contact deformation differentials between intact and ACL- deficient knee joints.

To test the intraobserver precision of the tibiofemoral cartilage thickness measurement using the MRI protocol and computer modeling, the cartilage layers that corresponded to the cutting planes were independently digitized 10 times by 3 observers (SKVdV, AH, and MK), with 1 day separating each re-segmentation. Cartilage thickness was determined at the 10 locations on each of the 8 cartilage cross-sections. The analyses were based on the

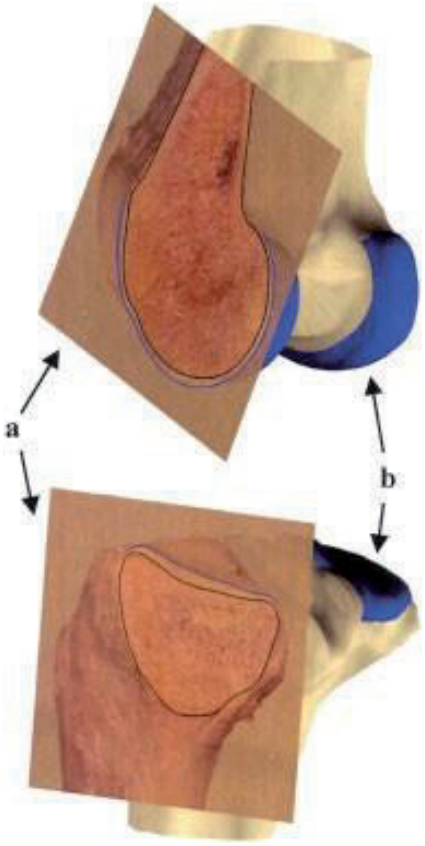

Figure A2. Comparison of direct measurement of the thickness of cartilage cross-sections from cadaver donors with measurement on MRI-based models. Digital images of osteotomies (**a**) were matched to the respective cross-sectional planes of the MRI models (**b**). The black (bone mesh) and blue (cartilage mesh) lines on the digital images indicate the intersection of the cartilage mesh models with the digital image at the location of the osteotomy. Only 2 cross-sections are shown.

maximum differences between the digitizations provided by each observer (results from the largest value minus the smallest value for each location). Intraobserver precision was assessed with Pearson's correlation coefficients and Student's t-tests of the paired differences of the observations. Correlations between the 10 digitizations were found to be excellent. Pearson's correlation coefficients for intraobserver precision at the measured locations were >0.984 ($P < 0.0001$) for each of the 3 readers.

Interobserver agreement was assessed by determining whether there were significant differences between the cartilage thickness measurements (thickness values from the first digitization session were selected) made by the 3 observers, using intraclass correlation coefficients (ICCs). Interobserver agreement was very high, with ICCs of 0.989–0.999 ($P < 0.0001$). These data are consistent with the values reported in the literature (49) and indicate that the cartilage thickness measurement using MRI-based cartilage models could be performed with great precision.